RSC Advances

ROYAL SOCIETY OF CHEMISTRY

www.rsc.org/advances

Inducting Effects of Ionic Liquid Crystals Modified-PEDOT:PSS on the Performance of Bulk Heterojunction Polymer Solar Cells

Xiaofeng Wang[1], Siwei Hu[1], Qiujuan Li[1], Fan Li[*1], Kao Yao[2], Meiying Shi[3]

[1]Department of Materials Science and Engineering, Nanchang University, 999 Xuefu Avenue, Nanchang 330031, China; [2]Institute of Photovoltaics, Nanchang University, 999 Xuefu Avenue, Nanchang 330031, China; [3]Wanfu Middle School, Ji'an 343100, Jiangxi Province, China

Abstract

A kind of ionic liquid crystals, 4′-(N, N, N-trimethyl ammonium bromide hexyloxy)-4-cyanobiphenyl (6CNBP-N), was synthesized and explored as a novel additive to modify the PEDOT:PSS anode buffer layer for P3HT:PCBM polymer solar cells (PSCs). Due to the ionic functions of 6CNBP-N, the amount of PEDOT on top surface of PEDOT:PSS was increased as increasing the amount of 6CNBP-N, leading to rougher surface and better conductivity. Most strikingly, when the 6CNBP-N modified PEDOT:PSS anode buffer layer was annealed at 150 ℃ (in the mesophase temperature region of 6CNBP-N), the more continuous network in the modified PEDOT:PSS film and more ordered microstructure and higher crystallization of P3HT in the overlying P3HT:PCBM active layer were formed, mainly induced by the self-assembling behavior of 6CNBP-N in its mesomorphism, and thus favoring excition dissociation, charge transport and collection. Without undergoing the annealing of active layers, the power conversion efficiency (PCE) of 3.17% was obtained. Our results showed that the ionic liquid crystals, which combined the liquid crystal properties and ionic functions, was a promising additive for PEDOT:PSS, which could improve the properties of PEDOT:PSS buffer layer and the overlying active layer at the same time, thereby enhancing the PCE of PSCs.

Keywords: Polymer solar cell; PEDOT:PSS; Ionic liquid crystal

[*] Corresponding author. Tel: +86 791 83969553; fax: +86 791 83969329. *E-mail address*: lfan@ncu.edu.cn (F. Li)

1. Introduction

Bulk-heterojunction (BHJ) polymer solar cells (PSCs) have attracted extensive research and development due to their advantages of low cost, light weight, flexibility, and ease of fabrication compared to the conventional inorganic solar cells.[1-3] In the past few years, significant progress with power-conversion-efficiency (PCE) over 9% has been made by the application of high performance BHJ material systems and device structures.[4] BHJ polymer solar cells are commonly composed of a blend layer of a conjugated-polymer donor (such as poly(3-hexylthiophene), P3HT) and a fullerene-derivative acceptor (such as phenyl-C_{61}-butyric acid methyl ester, $PC_{61}BM$) sandwiched between a transparent indium tin oxide (ITO) electrode and a metal electrode.[5] Many factors influence the performance of PSCs, including the absorption properties of the active layer, the work functions of the electrodes, and the morphology and charge carrier mobility in the active layer, etc. Recently, many efforts are focused on the optimization of buffer layers to improve device performance and the results show that buffer layers play an important role in PSCs and have been frequently used to control the injection conditions, converting blocking contacts into ohmic contacts in some cases.

Poly(3,4-ethylenedioxythiophene):poly(styrenesulfonate) (PEDOT:PSS) is an important anode buffer layer in PSCs mainly due to its virtue of high visible light transmittance, excellent thermal stability, good mechanical flexibility and solution-based fabrication process.[6-9] On the other hand, PEDOT:PSS buffer layer can enhance the hole transport from the active layer into the ITO anode due to its higher work function that can lower the energy barrier at the interface of ITO/active layer. However, the poor electrical conductivity of PEDOT:PSS films arising from the insulating species (i.e., PSS) limits the performance improvement of PSCs mainly due to the increase of series resistance.[10] Thus, different solvents or additives, such as ethylene glycol (EG), ethanol, 2-propanol, dimethyl sulfoxide (DMSO), acetonitrile, tetrahydrofuran, carbon nanotubes, bromine, etc, are added into the aqueous dispersion of PEDOT:PSS to modify the morphology and enhance the electrical

conductivity of PEDOT:PSS films, hence improve the performance of the device.[11-16] Although numerous reports have been published on optimizing the conductivity of PEDOT:PSS buffer layer to enhance the PCE of PSCs, few studies pay attention to the effects of the modified PEDOT:PSS interface on the active layers characteristics.[17] Specifically, it should be ideal that active layers microstructure, as well as PEDOT:PSS properties, are improved at the same time by incorporating an additive to the PEDOT:PSS.

Recently, ionic liquid crystals (ILCs), the combination of liquid crystal (LC) and ionic liquid (IL), have attracted intense interest because of their dual behavior, such as low melting temperature, ionic conductivity, thermal stability and polarity originated from typical ionic liquid materials in conjunction with the molecular orientational order from liquid crystals. Self-organized ILCs nanomaterials that exhibit electronic and ionic functions can be obtained by association of π-conjugated molecules having ionic moieties.[18-21] Moreover, our previous works have shown that the biphenyl conjugated mesogens can induce the crystallization and ordering of conjugated polymer chains, especially upon mesophase annealing, and hence improve the carrier mobility.[22] In addition, Fang et al. reported that the PEDOT:PSS modified with a kind of cationic surfactant, N,N,N-trimethyl-1-hexadecanaminiu bromide (CTAB), not only enhanced the contact between PEDOT:PSS films and the active layer, but also favored P3HT crystallization and phase segregation with PCBM in the active layer.[17]

Bearing this in mind, herein, we rationally designed and synthesized a novel ILCs composed of biphenyl mesogens and the same cationic groups as CTAB, 4′-(N, N, N-trimethyl ammonium bromide hexyloxy)-4-cyanobiphenyl (**6CNBP-N**), which combine the properties of liquid crystals ordering and ionic liquids compatible with water and organic substance. Our intention is to develop a new additive for PEDOT:PSS which not only can enhance the morphology and electrical conductivity of PEDOT:PSS, but also can improve the active layer microstructure. In the present paper, we fabricate the PSCs based on P3HT:PCBM by application of

6CNBP-N-modified PEDOT:PSS as the anode buffer layer [chemical structures of PEDOT:PSS and 6CNBP-N and device structure of PSCs are shown in **Figure 1**] and investigate the effect of the modified PEDOT:PSS on the photovoltaic performance of the PSCs. In details, an investigation is taken to understand the influence of the doping amount and liquid crystal behavior of 6CNBP-N on the morphologies and conductivity of PEDOT:PSS films, along with liquid crystals inducting effect on the above P3HT:PCBM blend morphology, and finally on the performance characteristics of the resultant devices.

------Figure 1------

2. Experimental

2.1 Synthesis of ionic liquid crystals 4′-(N, N, N-trimethyl ammonium bromide hexyloxy)-4-cyanobiphenyl (6CNBP-N)

The synthesis route to ionic liquid crystal, 4′-(N, N, N-trimethyl ammonium bromide hexyloxy)-4-cyanobiphenyl (6CNBP-N), is outlined in the **Scheme S1**. 4′-(n-bromoalky) biphenyl-4-carbonitrile was prepared according to our previously reported method.[23] The second step was carried out according to a reference method (Detailed experimental see Supporting Information).[24] The obtained compound was characterized by ^{1}H nuclear magnetic resonance (^{1}HNMR) and Fourier transform infrared (FT-IR) spectroscopy, see **Figure S1** and **Figure S2**.

2.2 The modification of PEDOT:PSS using 6CNBP-N

The treatment of ionic liquid crystal 6CNBP-N on PEDOT:PSS was performed by dissolving 6CNBP-N in 2-propanol and methanol and then the 6CNBP-N solution was mixed with PEDOT:PSS (Baytron PAl4083). We optimized the amount of 6CNBP-N (0.4, 1.0, 1.2 and 1.5 mg) in 500 μL 2-propanol and 200 μL methanol, which were then mixed with 350 mL of PEDOT:PSS.

2.3 Device fabrication

The devices were prepared on top of pre-patterned ITO glass substrate. The substrates were cleaned by ultrasonic treating for 20 min in acetone followed by deionized water and then 2-propanol. The substrates were dried under a stream of nitrogen and subjected to the treatment of UV-ozone over 10 min. A filtered dispersion of the 6CNBP-N-modified PEDOT:PSS anode buffer layer was then spin coated onto clean ITO substrates at 4000 rpm for 60 s, which were subsequently baked at different temperature for 10 min to remove residual water. For comparison, the unmodifed PEDOT:PSS film was annealed at 150 ℃ for 10 min, named as the pristine PEDOT:PSS. The thickness of anode buffer layer is about 40 nm. After cooling to ambient temperature in a nitrogen-filled glovebox, the P3HT:PCBM films were spin-coated (1000 rpm for 60 s) onto the anode buffer layers from solutions where P3HT:PCBM (1:1 w/w) were mixed together in dichlorobenzene with the concentration of P3HT and PCBM are both 10 mg/ml for 100 nm thick layers and stirred overnight at 60 ℃ before use. Subsequently, LiF (0.6 nm) and Al (100 nm) electrodes were deposited via thermal evaporation in vacuum ($<10^{-6}$ Torr) in thickness of approximately. Current–voltage (J–V) characteristics were recorded using a Keithley 2400 Source Meter under 100 mW/cm^2 simulated AM 1.5G irradiation (Abet Solar Simulator Sun2000). All the measurements were performed under ambient atmosphere at room temperature.

2.4 Characterizations

The ^{1}H nuclear magnetic resonance (^{1}HNMR) spectra were collected on a Bruker ARX 400 NMR spectrometer with deuterated chloroform as the solvent and with tetramethylsilane (δ=0) as the internal standard. The FT-IR spectra are recorded on a Shimadzu IRPrestige-21 Fourier transform infrared spectro-photometer by using KBr substrates. The ultraviolet–visible (UV-vis) spectra of samples were recorded on a Hitachi UV-3010 spectrophotometer. Thermogravimetric analysis (TGA) was performed on a PerkinElmer TGA 7 for thermogravimetry at a heating rate of 20 ^{o}C/min under nitrogen. Differential scanning calorimetry (DSC) was used to determine phase-transition temperatures on a Perkin-Elmer DSC 7 differential

scanning calorimeter with a constant heating/cooling rate of 10 ℃/min. Texture observations by polarizing optical microscopy (POM) were made with a Nikon E600POL polarizing optical microscope equipped with an Instec HS 400 heating and cooling stage. The X-ray diffraction (XRD) study of the samples was carried out on a Bruker D8 Focus X-ray diffractometer operating at 30 kV and 20 mA with a copper target (λ =1.54 Å) and at a scanning rate of 1^{o}/min. Transmission electron microscopy (TEM) images were recorded using a JEOL-2100F transmission electron microscope and an internal charge-coupled device (CCD) camera. Atomic force microscopic (AFM) images were measured on a nanoscope III A (Digital Instruments) scanning probe microscope using the tapping mode. The surface resistance of each PEDOT:PSS film was evaluated using four-point-probe measurements (NAPSON/Cresbox/RT-80).

3. Results and discussion

6CNBP-N is a kind of ionic liquid crystals which combine the liquid crystal properties and ionic functions. The mesomorphic behavior of 4′-(N, N, N-trimethyl ammonium bromide hexyloxy)-4-cyanobiphenyl (6CNBP-N) has been studied by polarizing optical microscopy (POM) and differential scanning calorimetry (DSC) (**Figure 2**). The 6CNBP-N exhibits two discrete endotherm transitions at 97.3 ℃ and 165.3 ℃ on first heating scan in DSC curves. The first transition corresponds to the solid-mesophase transition, and the second corresponds to the mesophase-isotropic transition. Thus the thermotropic enantiotropic mesophase of 6CNBP-N is between 97.3 and 165.3 ℃. The 6CNBP-N exhibits optical anisotropy when observed by POM at 150 ℃ during cooling from melt state, suggesting that the cyano-biphenyl mesogens endow the compound with thermotropic liquid-crystalline behavior. The thermal stability of 6CNBP-N has been investigated by thermogravimetric analysis (TGA) (**Figure S3**). The 6CNBP-N begins to decompose at about 245 ℃ and loses most of the weight at about 380 ℃, showing good thermal stability.

------Figure 2------

Firstly, we investigate the influence of the doping amount of 6CNBP-N on the morphology, optical transmittance and conductivity of PEDOT:PSS films. All films are annealed at 150 ℃ for 10 min in air. As we know, the surface morphology of the PEDOT:PSS buffer layers will influence the photovoltaic performance of the PSCs. Therefore, the effect of 6CNBP-N modification on the surface morphology of PEDOT:PSS layer is examined by atomic force microscope (AFM) technique in tapping mode, as displayed in **Figure 3**. And the root-mean-square (RMS) roughness of each film is also presented. The images of the pristine and modified PEDOT:PSS films all confirm a grain-like structure. The roughness for PEDOT:PSS layer without and with 0.4, 1.0, 1.2 and 1.5 mg 6CNBP-N are 0.98, 1.06, 1.08, 1.16, 1.17 nm, respectively. It can be observed that the surface roughness increases with increasing the 6CNBP-N concentration although the increase of roughness of PEDOT:PSS layer is actually rather small. The increased roughness arising from the 6CNBP-N modification might be due to the increased content of ILC or the increase in the amount of PEDOT on the surface of PEDOT:PSS films, attributing to the ionic function of 6CNBP-N similar to CTAB.[25,26] The same phenomena have also been observed by several other research groups.[17,26,27] The increased roughness likely increase the contact area between the PEDOT:PSS and the active layer, improving hole extraction to the anode. At the same time, rough surfaces may increase scattering of the incident light back into the active layer and hence lead to increased absorption.

------Figure 3------

As the light is incident from the ITO electrode and the PEDOT:PSS is used as an anode buffer layer on ITO, the optical transmittance of ITO/anode buffer layer plays an important role in the photon absorption in the device. **Figure 4(a)** shows the UV-visible transmittance spectra of the pristine and 6CNBP-N-modified PEDOT:PSS films. Compared with the pristine PEDOT:PSS, the 6CNBP-N-modified PEDOT:PSS

films exhibit somewhat lower transmittance intensity in overall trends. Meanwhile, the transmittance is dependent on the amount of 6CNBP-N doped in the PEDOT:PSS solution and as the amount of 6CNBP-N increases, the optical transmittance decreases. However, the change in transmittance among these films is not very significant and all simples show highly transparence with transmittance of above 85% in visible range (400-800 nm) except the obvious absorption at 300 nm, which is ascribed to biphenyl mesogen in 6CNBP-N.

In order to investigate the effects of doping 6CNBP-N on the electrical properties of the PEDOT:PSS films, corresponding surface resistance of films are evaluated using four-point-probe measurements. The surface resistance is measured from the average value of measurements on one sample for 5 times in ambient condition and the experimental error of film resistance measurement is about ±0.3 ohm/sq, shown in **Figure 4(b)**. It is obvious that the surface resistance decreases as the amounts of 6CNBP-N are increased until the 6CNBP-N doping amount exceeds 1.0 mg. The mechanisms of the improved conductivity in PEDOT:PSS through introduction of additives are still the debatable problem. In generally, electrical properties of conducting polymers are strongly related to the film morphology and chemical and physical structure. For PEDOT:PSS, complex and insulating PSS serves not only as a dispersant of PEDOT to make it soluble, but also as a charge-compensating counter-polyanion for the positively charged PEDOT backbone, forming on a molecular level the primary PEDOT:PSS structure.[9,28] As we have mentioned above, the 6CNBP-N modification increases the amount of PEDOT on the surface of PEDOT:PSS films, hence enhancing the conductivity. On the other hand, we also attribute this phenomenon to that 6CNBP-N liquid crystal molecules can improve the dispersion and uniformity of PEDOT:PSS. Considering the results of film morphology, optical transmittance and conductivity, the doping amount of 6CNBP-N in PEDOT:PSS has been optimized to 1.0 mg.

------Figure 4------

Apart from ionic properties, 6CNBP-N is also a kind of liquid crystal molecules. Therefore, in the next experiment, we will put particular emphasize on investigation of the liquid crystals inducting effects of 6CNBP-N on the performance of P3HT:PCBM BHJ PSCs. As the thermotropic enantiotropic mesophase of 6CNBP-N is between 97.3 and 165.3 ℃, we anneal the 6CNBP-N modified PEDOT:PSS anode buffer layers at 90 ℃ (below mesophase temperature), 150 ℃ (mesophase temperature) and 180 ℃ (above mesophase temperature) for 10 min, respectively. To eliminate the effect of active layer thermal annealing on 6CNBP-N modified PEDOT:PSS films and observe the inducting effects of 6CNBP-N liquid crystals more clearly, the P3HT:PCBM active layers are un-annealed. **Figure 5** displays the current-voltage characteristics of the photovoltaic devices under the illumination of AM 1.5G 100 mW/cm^2, and the performance parameters and the calculated values of series resistance (R_s) and shunt resistance (R_{sh}) are listed in **Table 1**. It can be seen that the photovoltaic performance is obviously improved for devices using 6CNBP-N modified PEDOT:PSS anode buffer layer compared with the pristine PEDOT:PSS. Moreover, it is noteworthy that different thermal annealing temperature of anode buffer layer mainly affects the short-circuit current density (J_{sc}) and fill factor (*FF*), with almost unchanged open-circuit voltage (V_{oc}). More interestingly, the best device performance is achieved when the modified PEDOT:PSS layer is annealed at mesophase temperature (150 ℃), with an increased J_{sc} (11.14 mA/cm^2), V_{oc} (0.63 V), and *FF* (45.1%) and a power conversion efficiency of 3.17%. At the same time, R_s of the device is decrease to 4.3 Ω cm^2 and R_{sh} is increase to 260.3 Ω cm^2 by utilizing modified PEDOT:PSS anode buffer layer annealed at 150 ℃. The enhancement of the J_{sc} and *FF* might be attributed to the increased charge separation and transport efficiency of the anode buffer layer. It also indicates that optimized P3HT:PCBM interpenetrate network may be formed due to the inducting effect of ionic liquid crystalline modified PEDOT:PSS. In addition, we also concern that after thermal annealing of PEDOT:PSS:6CNBP-N composite, the fraction of 6CNBP-N component

may be pushed to the film surface by PEDOT chain aggregation forces, where it may be absorbed by the P3HT:PCBM solution during spin-coating and therefore acting as an additive to the P3HT:PCBM active layer. For this reason, we have tried to perform a control experiment where 6CNBP-N is intentionally added as an additive to P3HT:PCBM blend. However, although 6CNBP-N contains biphenyl structure, it cannot dissolve into dichlorobenzene due to terminal ionic group (shown in **Figure S4**). Therefore, the control experiment is failed. Then we intend to further investigate the reason for the improvement of device performance by measurement of anode buffer layers micromorphology, active layer micro-structure and the crystallinity of polymer chain (*vide infra*).

------Figure 5------

AFM images are measured to investigate the influence of different annealing temperature on the surface morphology of the modified PEDOT:PSS film and the results are shown in **Figure 6**. The bright regions ascribe to PEDOT, whereas the dark regions denote the PSS. The RMS of the 6CNBP-N modified PEDOT:PSS annealed at 90, 150 and 180 ℃ is 1.12, 1.08 and 1.11 nm, respectively. It can be seen that there are no obvious difference among the surface roughness of the three samples. However, the smoother surface can be observed in the modified PEDOT:PSS film annealed at 150 ℃, mainly induced by the self-assembling behavior of ionic liquid crystal in its mesomorphism (**Figure 6b**). AFM results indicate that annealing treatment at mesophase temperature region of 6CNBP-N could improve charge transport across the PEDOT chain, which is consistent with the highest J_{sc} and *FF* value. For the device with 6CNBP-N modified PEDOT:PSS buffer layer annealed at 150 ℃, the maximum PCE is obtained, mainly due to the fact that it can reach the optimal balance between the dispersity in horizontal direction and the contact with active layer in vertical direction for PEDOT:PSS anode buffer layer. At the same time, the surface resistance of the 6CNBP-N modified PEDOT:PSS film under annealing treatment

before and after mesophase region, and in the mesophase region is also measured by the four-point probe technique. As expected, the surface resistance of the 6CNBP-N modified PEDOT:PSS films annealed at 90 ℃ (153.3 Ohm/sq) and annealed at 180 ℃ (150.0 Ohm/sq) increase compared with that of film annealed at 150 ℃ (149.0 Ohm/sq). The tendency of the surface resistance change is consistent with the tendency of the J_{sc} and PCE changes in the PSCs with different PEDOT:PSS modification layer.

------Figure 6------

As we know, the morphology of the active layer in PSCs plays a very important role in determining the PCE. Due to the limit of short exciton diffusion length in conjugated polymers, the polymer donor and acceptor need to form a bicontinuous networks at nanoscale for efficient exciton dissociation and charge collection.[29,30] TEM studies are performed to investigate the inducting effect of 6CNBP-N modified PEDOT:PSS on micro-structure of P3HT:PCBM film. TEM images of the un-annealed P3HT:PCBM blend films spin-coated on the pristine PEDOT:PSS and 6CNBP-N modified PEDOT:PSS layer annealed at different temperature for 10 min are shown in **Figure 7**. The P3HT:PCBM film spin-coated on the 6CNBP-N modified PEDOT:PSS layers under annealing treatment all demonstrate more uniform nanscale phase separation compared with P3HT:PCBM spin-coated on the pristine PEDOT:PSS layer. More importantly, obvious enhanced ordering of the blend morphology is presented in the bright-field TEM images of a P3HT:PCBM film on the modified PEDOT:PSS layers under annealing treatment in the mesophase region (150 ℃), see **Figure 7c**. And it indicates that the formation of the ordered microstructure is originated from the spontaneous assembly of the 6CNBP-N doped into the PEDOT:PSS anode buffer layer. The optimized micro-structure of active layer favors enhancement of the exciton dissociation and charge collection.

------**Figure 7**------

To validate the impact of the 6CNBP-N modified PEDOT:PSS films on the crystallinity of P3HT chain in the active layer, the ultraviolet-visible absorption spectra and XRD pattern of the un-annealed P3HT:PCBM films casted on the pristine PEDOT:PSS and modified PEDOT:PSS layers under various annealing treatment have been measured (**Figure 8**). As shown in **Figure 8(a)**, the P3HT:PCBM blend films on the 6CNBP-N modified PEDOT:PSS annealed at different temperature all display obvious red-shift and the vibronic absorption shoulder (at 605 nm) compared with that on the pristine PEDOT:PSS layer, revealing that the P3HT chain forms more ordered structure.[31] Especially, for the P3HT:PCBM blend film on the modified PEDOT:PSS annealed at 150 ℃, appearance of the optimal red-shift in absorption spectrum is observed and vibronic feature at 605 nm becomes more clear. However, when the annealing temperatures exceed the mesophase range (at 180 ℃), it would disrupt the tendency and get worse results, and the sample annealed at temperature below the mesophase temperature region (at 90 ℃) has the same phenomenon. This enhancement may be attributed to the inducting effect of 6CNBP-N in its liquid crystal state.[32] A red-shift in the more ordered P3HT film involves an enhanced conjugation length and therefore a shift of the absorption spectrum toward lower energy region appears,[33] which is further supported by the XRD pattern of P3HT:PCBM active layer shown in **Figure 8(b)**. Annealing temperature of 150 ℃ (mesophaes temperature) leads to an obvious increase in the intensity of the [100] diffraction peak ($2\theta = 5.4^{\circ}$), originating from the -lamellar packing of polymer chains along the crystallographic direction perpendicular to the backbone.[34,35] These results indicate that the 6CNBP-N modified PEDOT:PSS anode buffer layer can induce the crystallization of P3HT in the overlying active layer, especially, as the modified PEDOT:PSS annealed at liquid crystal state temperature, optimal result is obtained.

------**Figure 8**------

As the enhancement in photovoltaic properties can also be relate to charge transport, the impact of 6CNBP-N modified PEDOT:PSS anode buffer layer on the hole transport characteristics of devices based on un-annealed P3HT:PCBM as active layers has been assessed by measurement of hole-only device using Mott-Gurney space charge limited current (SCLC) model (**Figure 9**) and results are summarized in **Table 2**. The electron mobility can be characterized by the Mott-Gurney SCLC formula:[36]

$$J = (9/8)\mu_e\varepsilon_0\varepsilon_r(V^2/L^3)$$

Where J is the current density, μ_e is the electron mobility, ε_0 is the dielectric constant of the free space (ε_0=8.85 $\times 10^{-12}$ F m^{-1}), ε_r is the permittivity of active layer, V is the internal voltage in the device and L is the thickness of the active layer. The devices based on 6CNBP-N modified PEDOT:PSS anode buffer layers exhibit the improved hole-transport behaviors. Comparing with the pristine PEDOT:PSS as anode buffer layer, the hole mobility of devices with modified PEDOT:PSS layer increase one order of magnitude. More importantly, the hole mobility demonstrates the dependence on the annealing temperature of 6CNBP-N modified PEDOT:PSS layer. After thermal annealing treatment at mesophase temperature, the hole mobility increase to 2.95 $\times 10^{-3}$ cm^{2}V^{-1}s^{-1}. The improvement in hole mobility caused by 6CNBP-N modification originates from the improve morphology and conductivity of PEDOT:PSS anode buffer layers and micro-structure of active layers.

Conclusion

In summary, we have designed and synthesized the ionic liquid crystals, 4′-(N, N, N-trimethyl ammonium bromide hexyloxy)-4-cyanobiphenyl (6CNBP-N), and applied it as a novel additive to modify the properties of the PEDOT:PSS anode buffer layer and then to enhance the performance of polymer solar cells based on P3HT:PCBM. It is found that the conductivity and surface morphology of the PEDOT:PSS layer can be improved by the incorporation of 6CNBP-N. More importantly, the 6CNBP-N modified PEDOT:PSS can favor the P3HT crystallization

and induce ordered nano-scale phase separation of the P3HT:PCBM active layer, and thus to enhance charge transport and collection, especially in the case of the modified PEDOT:PSS annealed at mesophase temperature (150 ℃). Without any annealing treatment of P3HT:PCBM active layers, the PCE of PSCs reached 3.17%. Overall, the application of self-assembled ionic liquid crystalline for the modification of PEDOT:PSS can induce phase separation, crystallinity, and ordered structures of the active layers and paves a new way to enhance the photovoltaic performance of PSCs.

Acknowledgements

The authors acknowledge the financial support from the National Natural Science Foundation of China (51172103 and 61464006), Jiangxi Province Natural Science Foundation (20142BAB206007) and Jiangxi Province Young Scientist Project (20142BCB23002).

References

1 H. Y. Chen, J. H. Hou, S. Q. Zhang, Y. Y. Liang, G. W. Yang, Y. Yang, L. Q. Yu, Y. Wu, and G. Li, *Nat. Photonics.*, 2009, **3**, 649-653.

2 L. J. Huo, S. Q. Zhang, Xia Guo, Feng Xu, Yongfang Li, and Jianhui Hou, *Angew. Chem. Int. Ed.*,2011, **123**, 9871-9876.

3 Y. Y. Liang, Z. Xu, J. B. Xia, S. T. Tsai, Y. Wu, G. Li, C. Ray, and L. P. Yu, *Adv. Mater.*, 2010, **22**, E135-E138.

4 Z. C. He, C. M. Zhong, S. J. Su, M. Xu, H. B. Wu, and Y. Cao, *Nat. Photonics.*, 2012, **6**, 591-595.

5 G. Yu, J. Gao, J. C. Hummelen, F. Wudl, and A. J. Heeger, *Sci*, 1995, **270**, 1789-1791.

6 J. H. Park, T. W. Lee, B. D. Chin, D. H. Wang, and O. Ok Park, *Macromol. Rapid Commun.*, 2010, **31**, 2095-2108.

7 S. I. Na, S. S. Kim, J. Jo, and D. Y. Kim, *Adv. Mater.*, 2008, **20**, 4061-4067.

8 S. Kirchmeyer and K. Reuter, *J. Mater. Chem.*, 2005, **15**, 2077-2088.

9 L. Groenendaal, F. Jonas, D. Freitag, H. Pielartzik, and J. R. Reynolds, *Adv. Mater.*, 2000, **12**, 481-494.

10 K. KS, C. Y, L. HK, C. KY, and H. KJ, *Thin Solid Films*, 2009, **517**, 6096-6099.

11 Q. S. Wei, M. Mukaida, Y. Naitoh, and T. Ishida, *Adv. Mater.*, 2013, **25**, 2831-2836.

12 B. Peng, X. Guo, C. H. Cui, Y. P. Zou, C. Y. Pan, and Y. F. Li, *Appl. Phys. Lett.*, 2011, **98**, 243308.

13 Y. J. Xia, and J. Y. Ouyang, *J. Mater. Chem.*, 2011, **21**, 4927-4936.

14 T. Xiao, W. Cui, J. Anderegg, J. Shinar, and R. Shinar, Org. Electron., 2011, **12**, 257-262.

15 J. Park, A. Lee, Y. C. Yim, and E. Han, *Synthetic Metals*, 2011, **161**, 523-527.

16 J. Li, J. C. Liu, and C. J. Gao, *Journal of Polymer Science: Part B: Polymer Physics*, 2012, **50**, 125-128.

17 G. Fang, S. P. Wu, Z. Y. Xie, Y. H. Geng, L. X. Wang, *Macromol. Chem. Phys.*, 2011, **212**, 1846-1851.

18 S. Yazaki, M. Funahashi, and T. Kato, *J. Am. Chem. Soc.*, 2008, **130**, 13206-13207.

19 R. L. Kerr, S. A. Miller, R. K. Shoemaker, B. J. Elliott, and D. L. Gin, *J. Am. Chem. Soc.***,** 2009, **131**, 15972 -15973.

20 J. Motoyanagi, T. Fukushima, and T. Aida, *Chem. Commun.*, 2005, 101-103.

21 S. Yazaki, M. Funahashi, J. Kagimoto, H. Ohno, and T. Kato, *J. Am. Chem. Soc.*, 2010, **132**, 7702-7708.

22 K. Yao, Y. W. Chen, L. Chen, F. Li, X. E. Li, X. Y. Ren, H. M Wang, T. X. Liu, *Macromolecules*, 2011, **44**, 2698-2706.

23 F. Li, Q. J. Li, and Y. W. Chen, *Journal of Luminescence*, 2012, **132**, 2114-2121.

24 K. Yao, L. Chen, Y. W. Chen, F. Li, P. S. Wang, *J. Mater. Chem.*, 2011, **21**, 13780-13784.

25 M. D. obbelin, R. Marcilla, C. Tollan, J. A. Pomposo, J. R. Sarasua, and D. Mecerreyes, *J. Mater. Chem.*, 2008, **18**, 5354-5358.

26 J. S. Huang, P. F. Miller, J. S. Wilson, A. J. D. Mello, J. C. D. Mello, and D. D. C. Bradley, *Adv. Funct. Mater.*, 2005, **15**, 290-296.

27 C. J. Huang, J. C. Ke, W. R. Chen, T. H. Meen, and C. F. Yang, *Solar Energy Materials & Solar Cells*, 2011, **95**, 3460–3464.

28 O. P. Dimitriev, Y. P. Piryatinski, and A. A. Pud, *J. Phys. Chem. B*, 2011, **115**, 1357-1362.

29 S. S. van Bavel, E. Sourty, G. D. With, and J. Loos, *Nano Lett.*, 2009, **9**, 507-513.

30 D. Rauh, A. Wagenpfahl, C. Deibel, and V. Dyakonov, ***Appl. Phys. Lett.***, 2011, **98**, 133301.

31 Y. zhao, Z. Y. Xie, Y. Qu, Y. H. Geng, L. X. Wang, *Appl. Phys. Lett.*, 2007, **90**, 043504.

32 T. Y. Liu, H. C. Liao, C. C. Lin, S. H. Hu, and S. Y. Chen, *Langmuir*, 2006, **22**, 5804-5809.

33 G. Li, V. Shrotriya, J. Huang, Y. Yao, T. Moriarty, K. Emery, and Y. Yang, *Nat. Mater.*, 2005, **4**, 864-868.

34 T. J. Prosa, M. J. Winokur, J. Moulton, P. Smith, and A. J. Heeger, *Macromolecules*, 1992, **25**, 4364-4372.

35 M. He, L. Zhao, J. Wang, W. Han, Y. Yang, F. Qiu, and Z. Q. Lin, *ACS Nano*, 2010, **4**, 3241-3247.

36 X. G. Zhang, S. T. Pantelides, *Phys Rev Lett*, 2012, **108**, 266602.

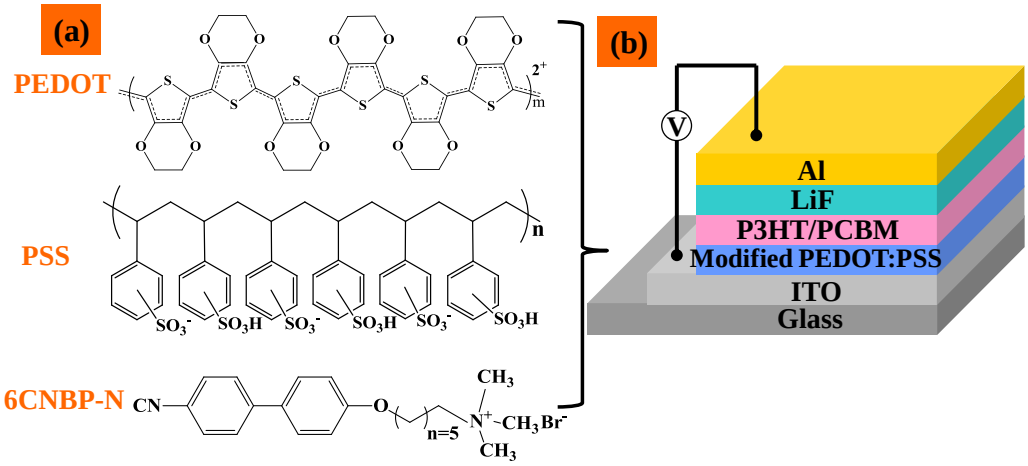

Figure 1. (a) Chemical structure of PEDOT:PSS and 6CNBP-N and (b) the device structure of the PSC.

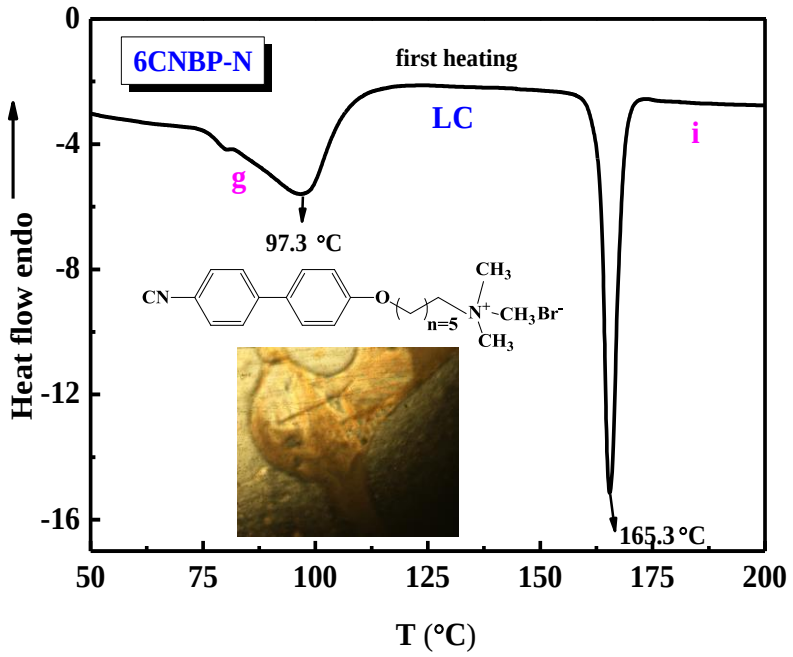

Figure 2. DSC thermogram of the 6CNBP-N recorded under nitrogen during first heating scans at a scan rate of 20 ℃/min. The inset shows the mesomorphic texture observed by POM at 150 ℃ during cooling from melt state (cooling rate: 1 ℃/min).

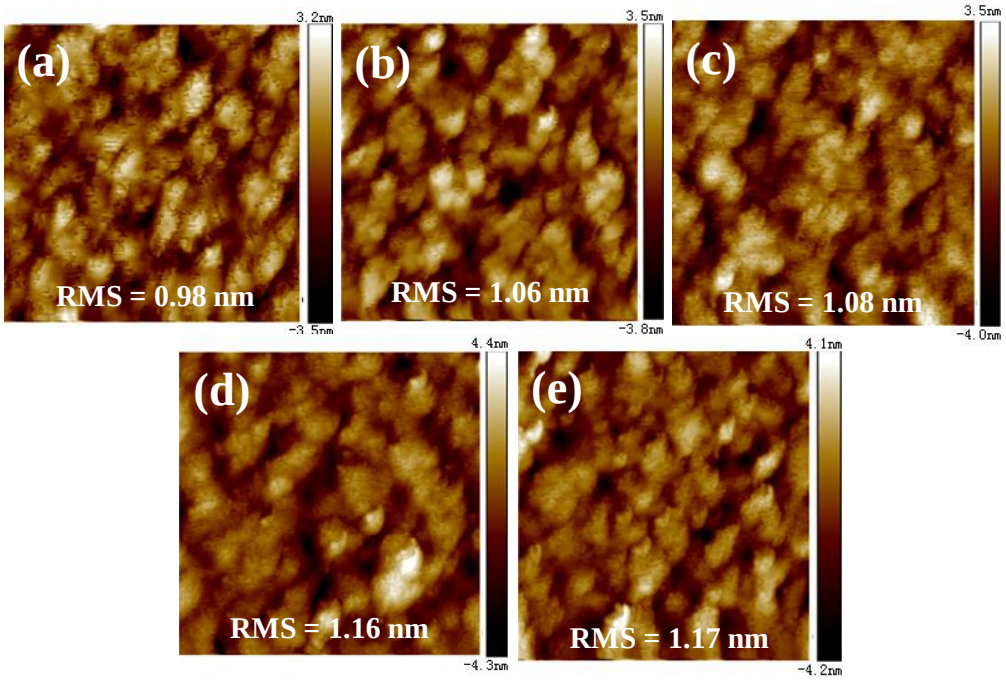

Figure 3. AFM topographic images of (a) pristine PEDOT:PSS film, (b-e) PEDOT:PSS films modified with different amount of 6CNBP-N (0.4 mg, 1.0 mg, 1.2 mg, 1.5 mg, respectively)

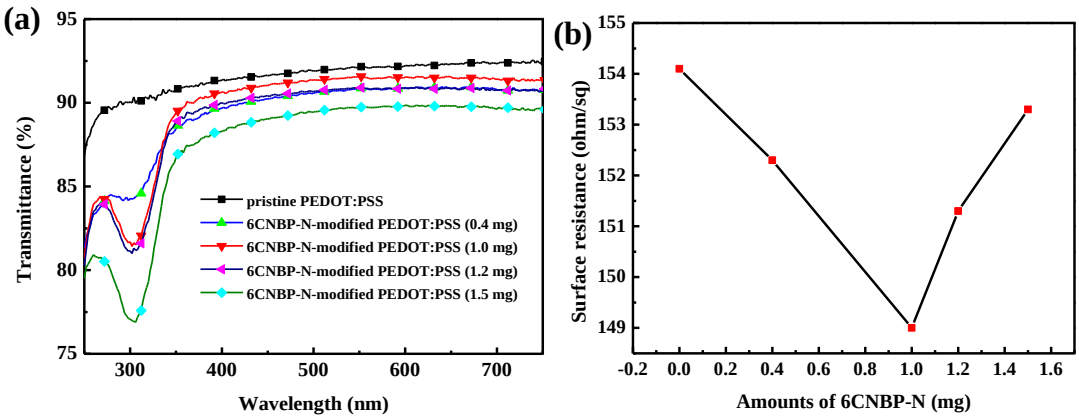

Figure 4. (a) UV-visible transmittance spectra and (b) surface resistance of PEDOT:PSS films modified with different amount of 6CNBP-N.

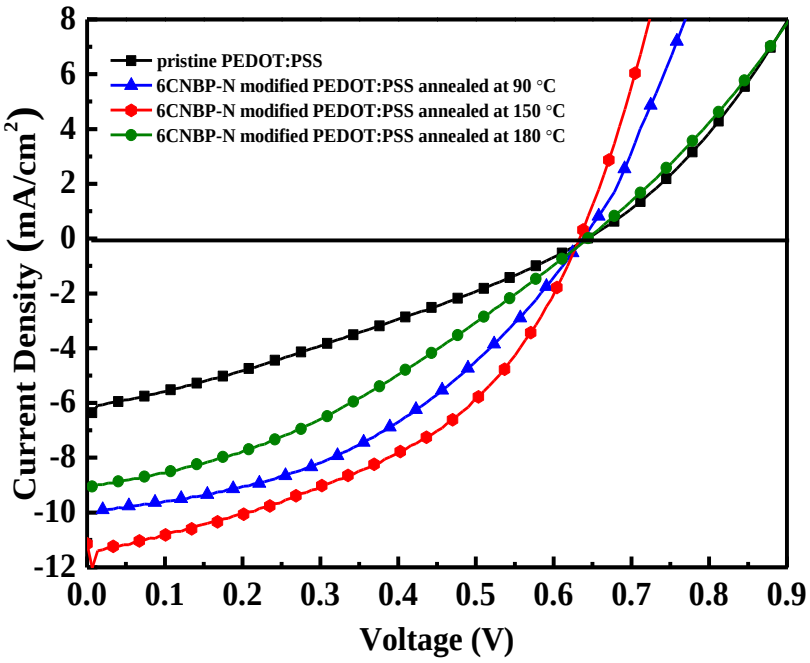

Figure 5. J-V characteristics of P3HT:PCBM polymer solar cells on pristine PEDOT:PSS and 6CNBP-N-modified PEDOT:PSS annealed at different temperature.

Table 1. Performance parameters of the devices based on P3HT:PCBM blends using the pristine PEDOT:PSS and 6CNBP-N-modified PEDOT:PSS annealed at different temperature as anode buffer layers.

Anode buffer layer	J_{sc} (mA cm^{-2})	V_{oc} (V)	FF (%)	R_s (Ω cm^2)	R_{sh} (Ω cm^2)	PCE (%)
Pristine PEDOT:PSS annealed at 150 ℃	6.36	0.64	29.4	19.5	140.0	1.20
modified PEDOT:PSS annealed at 90 ℃	9.90	0.64	42.4	8.4	191.1	2.68
modified PEDOT:PSS annealed at 150 ℃	11.14	0.63	45.1	4.3	260.3	3.17
modified PEDOT:PSS annealed at 180 ℃	9.05	0.64	35.0	17.6	147.3	2.04

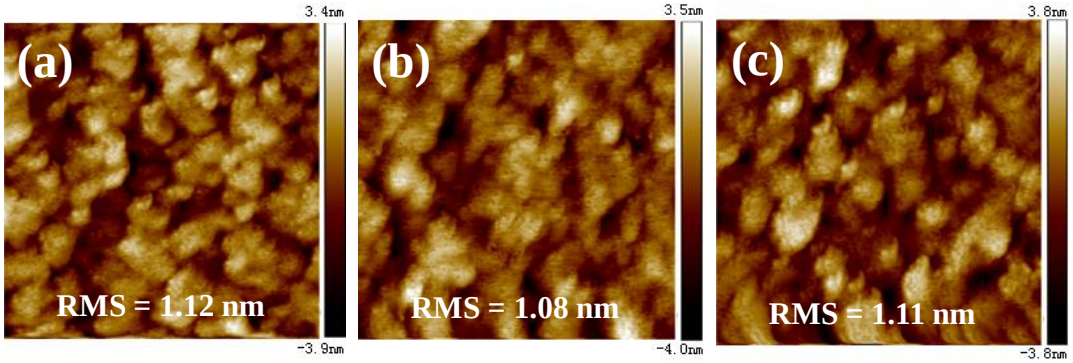

Figure 6. AFM topographic images of 6CNBP-N-modified PEDOT:PSS layers annealed at (a) 90 ℃, (b) 150 ℃ and (c) 180 ℃.

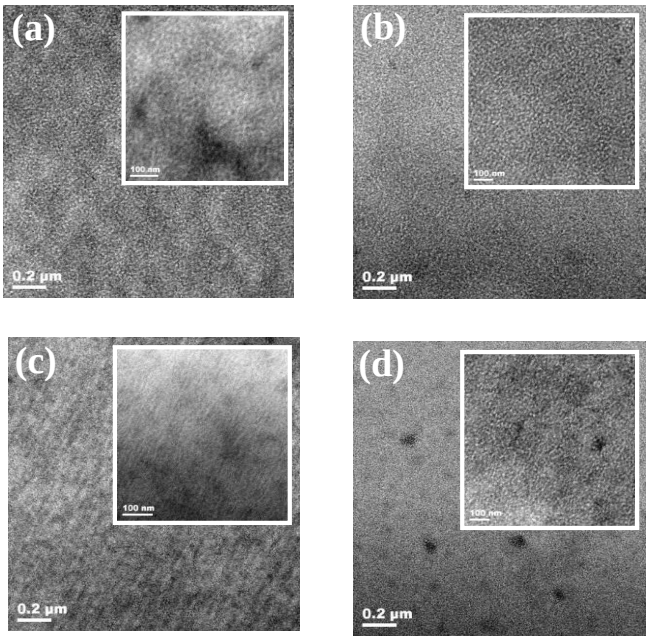

Figure 7. TEM images of un-annealed P3HT:PCBM blend films on the (a) pristine PEDOT:PSS and 6CNBP-N-modified PEDOT:PSS annealed at (b) 90 ℃, (c) 150 ℃, (d) 180 ℃.

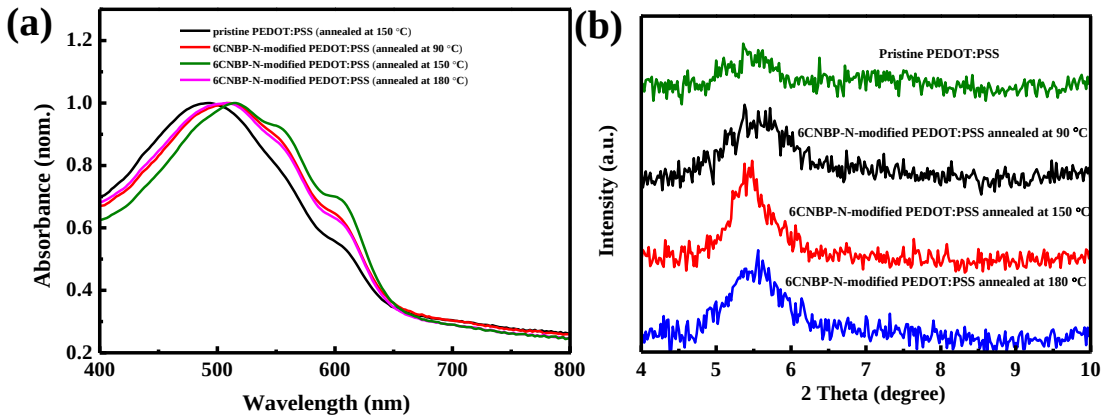

Figure 8. (a) Ultraviolet-visible absorption spectra and (b) XRD patterns of the un-annealed P3HT:PCBM blend films on the pristine PEDOT:PSS and 6CNBP-N-modified PEDOT:PSS annealed at 90 ℃, 150 ℃ and 180 ℃, respectively.

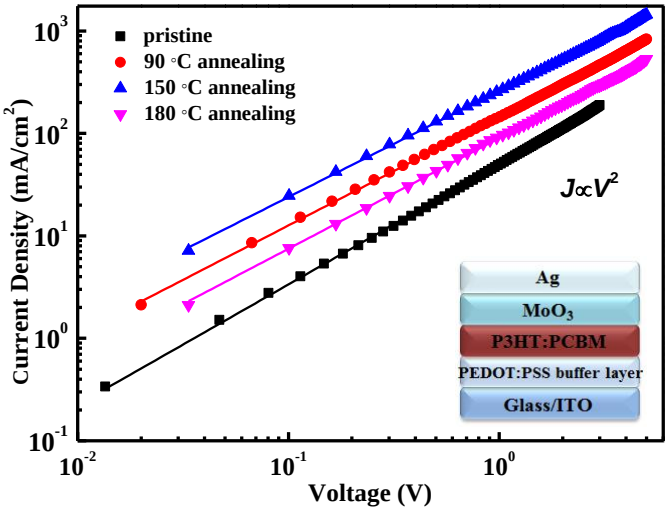

Figure 9. Log *J vs.* log *V* plots for Mott–Gurney SCLC fitting of the hole-only devices using pristine and 6CNBP-N-modified PEDOT:PSS annealed at different temperature, and the inset was the architecture of hole-only device.

Table 2. hole motilities (μ_h) of P3HT:PCBM deposited on the pristine PEDOT:PSS and 6CNBP-N modified PEDOT:PSS annealed at different temperature based on hole-only devices.

Annealing temperature	pristine	90 ℃	150 ℃	180 ℃
μ_h ($cm^2 V^{-1}s^{-1}$)	5.66×10^{-4}	1.65×10^{-3}	2.95×10^{-3}	1.02×10^{-3}

Table of content:

Inducting Effects of Ionic Liquid Crystals Modified-PEDOT:PSS on the Performance of Bulk Heterojunction Polymer Solar Cells

Xiaofeng Wang, Siwei Hu, Qiujuan Li, Fan Li*, Kao Yao, Meiying Shi

Photovoltaic performance was improved in P3HT/PCBM bulk-heterojunction solar cells induced by ionic liquid crystals modified PEDOT:PSS anode buffer layer.